

Experimental Maintenance of Chaos

Visarath In,¹ Susan E. Mahan,¹ William L. Ditto,¹ and Mark L. Spano^{2,1}

¹*Applied Chaos Laboratory, School of Physics, Georgia Institute of Technology, Atlanta, Georgia 30332*

²*Naval Surface Warfare Center, Carderock Division, Silver Spring, Maryland 20903*

(Received 25 January 1995)

We present a method for the anticontrol or maintenance of chaos designed for easy application to physical and biological systems. The method is based on the return map of the experimental data and requires only small, very infrequently applied time-dependent perturbations of a single system parameter and does not require any model equations for or *a priori* knowledge of the system dynamics. The method is shown to be able to reliably sustain chaos in a magnetomechanical ribbon experiment.

PACS numbers: 05.45.+b, 75.80.+q

Since Ott, Grebogi, and Yorke (OGY) [1] published their paper on the theory of the control of chaos, a major thrust of the work in experimental chaos has been to convert the chaos found in various physical systems into periodic motion. Since the experimental control of chaos was first demonstrated [2] in a mechanical system (a magnetoelastic ribbon), the control of chaos has been implemented in lasers [3], electronic circuits [4], chemical reactions [5], and biological systems [6,7]. Although chaos control may be very advantageous in many systems [8], it has been suggested that pathological destruction of chaotic behavior (possibly due to some underlying disease) may be implicated in heart failure [9] and some types of brain seizures [7]. Thus some systems may require chaos and/or complexity in order to function properly. Another situation in which the maintenance of chaos might be useful is the mixing of fluids [10]. Experimental work by Schiff *et al.* [7] demonstrated an *ad hoc* method for increasing the complexity (decreasing the periodicity) of an *in vitro* hippocampal rat brain slice preparation. Recent theoretical and computational work by Yang *et al.* [11] indicates that intermittent chaotic systems can be made to exhibit continuous chaotic behavior (no intermittent periodic episodes).

The main contribution of this Letter is a general theoretical method for the maintenance of chaos, which is then implemented experimentally in a magnetomechanical system demonstrating intermittency [12]. This intermittency appears as chaos interspersed with long periodic episodes. This method is readily applicable to experiment and relies only on experimentally measured quantities for its implementation.

As opposed to the *ad hoc* method for increasing the complexity implemented by Schiff *et al.* [7] (which they term anticontrol), the method of chaos anticontrol proposed by Yang *et al.* [11] is based on the observation that a map-based system in a regime of transient chaos, such as that near a transition periodicity into chaos, has special regions in its phase space that they term "loss regions." If the system enters such a region it immediately ceases its chaotic motion. Yang *et al.* [11] identify these regions

along with n preiterates of each loss region. If the system enters a preiterate, they apply a small perturbation to an accessible system parameter in order to interrupt the progression of the system toward a loss region. The perturbation places the system in a region of phase space that is neither a loss region nor a preiterate of one. This requires explicit knowledge of the map of the system and is accordingly difficult to accomplish. Thus the lack of generality of the Schiff method and the difficulty of experimental implementation of the Yang method are the motivation for the present work.

We propose a general anticontrol method that is more readily applicable to experiment and that relies only on experimentally measured quantities for its implementation. To start we make only the following assumptions about the system: (1) the dynamics of the system can be represented as an n -dimensional nonlinear map (e.g., by a surface of section or a return map) such that points or iterates on such a map are given by $\vec{\xi}_n = \vec{f}(\vec{\xi}_{n-1}, p)$, where p is some accessible system parameter; (2) there is at least one specific region of the map (termed a loss region) that lies on the attractor into which the iterates will fall when making the transition from chaos to periodicity; and (3) the structure of the map does not change significantly with small changes $\delta p \equiv p - p_0$ in the control parameter p about some initial value p_0 .

On the return map derived from a system, the locations of loss regions are determined by observing immediate preiterates of undesired points which correspond to periodic orbits. Clusters of these preiterates are identified as the loss regions. The extent of each loss region is determined by the distribution of points in that region (Fig. 1). The time evolution of each region may be traced back through m preiterates, as desired.

Next, in a fashion similar to the OGY chaos control method [1], we change p slightly, observing the resulting change in each loss region's location, and estimate the local shift of the attractor \vec{g} for each loss region with respect to a change in p as follows:

$$\vec{g} = \frac{\partial \vec{f}(\vec{\xi}_n, p)}{\partial p} \approx \frac{\Delta \vec{f}(\vec{\xi}_n, p)}{\Delta p}.$$

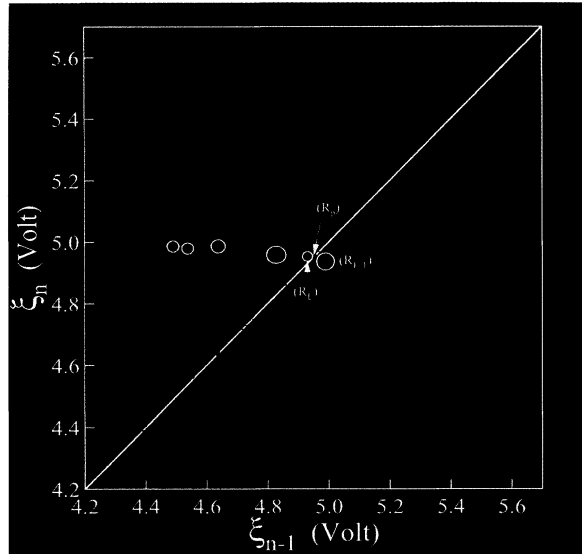


FIG. 1. Return map constructed from experimental data showing the loss region and its preiterates (circles). Region (R_L) denotes the loss region, region (R_{L-1}) denotes the first preiterate of the loss region going back in time, and region (R_p) denotes the period 1 orbits clustering on the diagonal of the map. The other four circles denote the (R_{L-m}) preiterate regions. Any orbit that falls into any one of the R_{L-m} regions will proceed directly into the R_{L-1} region and then proceed onto the loss region followed by the unwanted periodic orbit.

As an approximation we take \vec{g} to be the same for all loss regions on the attractor for sufficiently small parameter changes δp (otherwise calculation of \vec{g} for each loss region is required). This is not strictly necessary in order to implement the method but is simply a convenience that is approximately true for many systems (including our magnetoelastic ribbon) and for small δp 's.

Anticontrol can be applied once the system has entered the m th preiterate of the loss region. Since the map is constructed as a return map (or delay coordinate embedding) with ξ_n vs ξ_{n-1} , the y coordinate of the n th point becomes the x coordinate of the $(n+1)$ st point. Since we know the x coordinate of the next point and the *size* of the region that this $(n+1)$ st point would normally fall into, we calculate a minimum distance that we must move the attractor so that this next point falls outside of that region. This distance d is translated into the appropriate parameter change δp by $\delta p_n = d_{n+1}/|\vec{g}|$, where the direction of the motion is along \vec{g} .

If each of the m preiterates of the loss region is circumscribed by a circle of radius r_m (the worst case), we have $\delta p_n = 2r_m/|\vec{g}|$ where it is understood that the $(n+1)$ st point falls into the m th preiterate region. This is the maximum perturbation needed to achieve anticontrol and guarantees that the next point will fall outside the m th preiterate region by moving the point one full diameter of the circle surrounding the loss region. We can improve upon

this worst case. With a return map, we know the x coordinate of the next point. Because we have the choice of whether to apply the perturbation in either the positive or the negative \vec{g} direction, we can select the sign of the perturbation to move the next point to the left if this x coordinate is in the left half of the preiterate region and vice versa. Thus the minimum distance to move is reduced to r_m and, consequently, $\delta p_n = r_m/|\vec{g}|$, a significant reduction in the strength of the perturbation.

Additionally, if the shape of the preiterate region of interest is approximately linear (linelike) and its slope is perpendicular to \vec{g} , then d is at most r_m and may approach the thickness of this linear segment ($\delta p_n \ll r_m/|\vec{g}|$). Thus, while not necessary to achieve anticontrol, a detailed knowledge of the *shape* of the loss region and its preiterates can further reduce the size of the perturbation required to achieve anticontrol.

The experimental system [13] consists of a gravitationally buckled magnetoelastic ribbon driven parametrically by a sinusoidally varying magnetic field. The ribbon is clamped at its lower end and its position is measured at a point a short distance above the clamp. The Young modulus of the ribbon can be varied by more than a factor of 10 by application of an external magnetic field. We apply an ac magnetic field of amplitude H_{ac} and frequency f added to a dc field of amplitude H_{dc} , such that $H_{applied}(t) = H_{dc} + H_{ac} \sin(2\pi ft)$. We choose $f = 0.95$ Hz, $H_{ac} = 0.961$ Oe, and $H_{dc} = -1.221$ Oe in order to put the system in a state of intermittent chaos. We construct a return map by measuring the position ξ_n of a point on the ribbon once every driving period and by then plotting the current position ξ_n vs ξ_{n-1} .

On the return map, we identify the loss region and its preiterates (circles in Fig. 1). The loss region (R_L) is denoted by the circle just to the left of the diagonal. Its first preiterate (R_{L-1}) lies to the right of the diagonal. The other circles denote earlier preiterates (R_{L-m}). Points that enter any of these regions will eventually go to the region R_{L-1} . Once there they will proceed into the loss region R_L on the next iterate. Then the system becomes periodic. This appears as a cluster of points (R_p) on the diagonal of the map. The points that enter the preiterate regions mediate the intermittent transition from chaos to periodicity [12]. During anticontrol we apply a perturbation when an orbit enters the region R_{L-1} so that the next orbit will fall out of R_L .

The extent of the m th preiterate region is determined by observing the set of points that after m iterations fall into the loss region, as well as neighboring points that do not fall into the loss region after m iterations. The boundary of the loss region lies between these points. The \vec{g} vector is determined by changing p_0 by ± 0.0068 Oe. As illustrated in Fig. 1, the two loss regions are very close to the cluster denoting the periodic orbit. Rarely during anticontrol the orbit is kicked into the period 1 region. This requires us on the succeeding iteration to implement anticontrol for the periodic region as well in

order to safeguard against the system remaining there. Of course when this happens a somewhat larger perturbation will be required to move the system away from this periodic orbit. A value of 0.0237 Oe is adequate to control this problem in this experiment. A more elegant but computationally difficult solution would be to choose the original perturbation so that it avoids all of the loss regions and preiterates. Though this is possible, we chose not to implement it here.

Figure 2(a) shows the results of the anticontrol. The first 10 000 iterates are run with anticontrol turned off. During this time, the system intermittently switches between chaos and the period 1 motion. Once the anticontrol is turned on, the periodic behavior is eliminated for over 32 000 iterates. When the anticontrol is turned off, the periodic behavior reappears. The corresponding anticontrol perturbations are shown in Fig. 2(b). The nominal dc magnetic field is -1.221 Oe. During anticontrol the largest perturbation is 1.106% of this value ($\delta p_{\max} = 0.020$ Oe). Significantly the anticontrol signal needed to be applied *only* 0.12% of the time to keep the system chaotic.

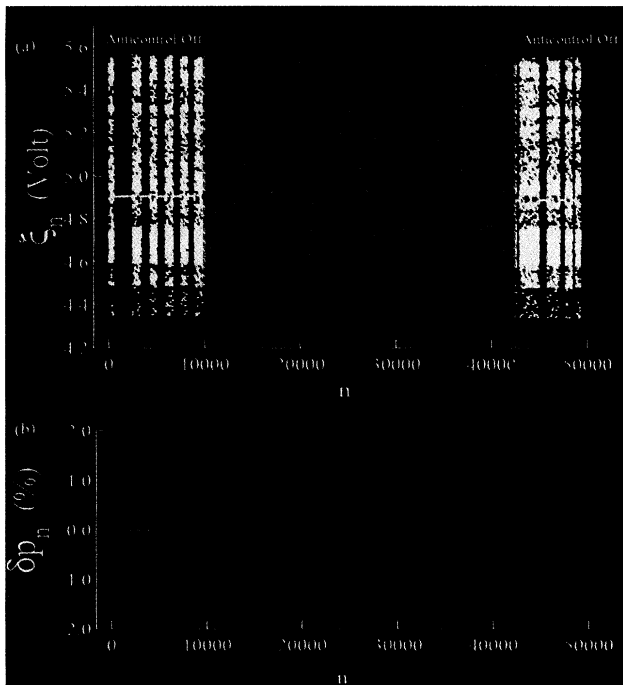


FIG. 2. (a) Time series from experimental data showing the system before, during, and after anticontrol. The dashed vertical lines separate the different regions. Before and after anticontrol, the system is switching between chaos and periodicity (laminar phase). With the perturbations applied during anticontrol, the system is rid of laminar phases. (b) Perturbations applied to achieve anticontrol. Their magnitudes are expressed as a percentage of the nominal dc magnetic field of -1.221 Oe. $\delta p_{\max} = 1.106\%$ and the fraction of time with $\delta p \neq 0$ is 0.0012.

The efficacy of the method is shown in Fig. 3. The first pane shows a probability histogram of the time series data for the unperturbed system. The large narrow peak near $x = 4.95$ reflects the fact that the system spends most of the time in a period 1 orbit. (Note the *logarithmic* vertical scale.) Contrast this with Fig. 3(b), where the anticontrol has been applied. The strong peak has been eliminated, and its probability has been spread over the rest of the x values with a distribution that approximates the original distribution of the intermittent chaotic data.

The effect of the anticontrol may be qualitatively appreciated by looking at Fig. 4. The 3D histogram in Fig. 4(a) reflects the density of points over the attractor (return map, Fig. 1) of the unperturbed system. (Note that the vertical scale here is *linear*.) Most of the probability resides in the strong central peak that represents the period 1 orbit. The density of the points resulting from anticontrol is presented in Fig. 4(b). Here the probability is spread over the entire chaotic part of the attractor with a distribution that approximates that of the chaotic parts of the unperturbed intermittency chaotic system.

Note that there is still a period 1 peak in Fig. 4(b). This represents a period 1 motion that *does not destroy the chaos*. The anticontrol prevents only the period 1 motion initiated by following the sequence of preiterates that leads to the loss region and subsequently to the loss of chaoticity. However, the method does *not* interfere with sequences of points that enter the loss region by other routes and that do not destroy the chaos. This period 1 motion is *naturally* unstable and is properly one of the

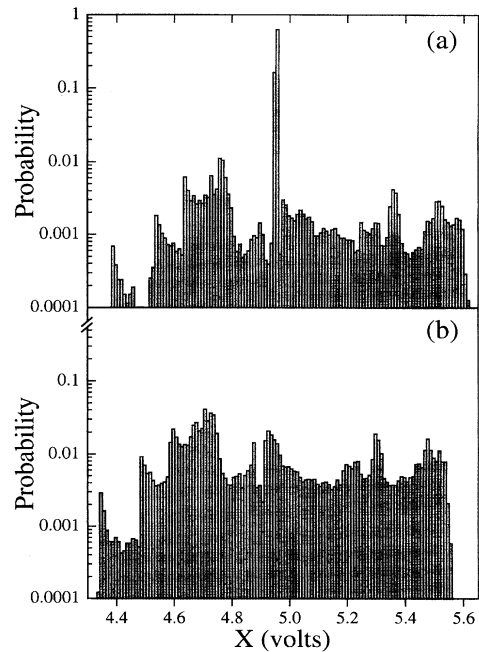


FIG. 3. Histograms of the time series data of (a) the unperturbed and (b) the anticontrolled data. Note that the vertical scales are logarithmic.

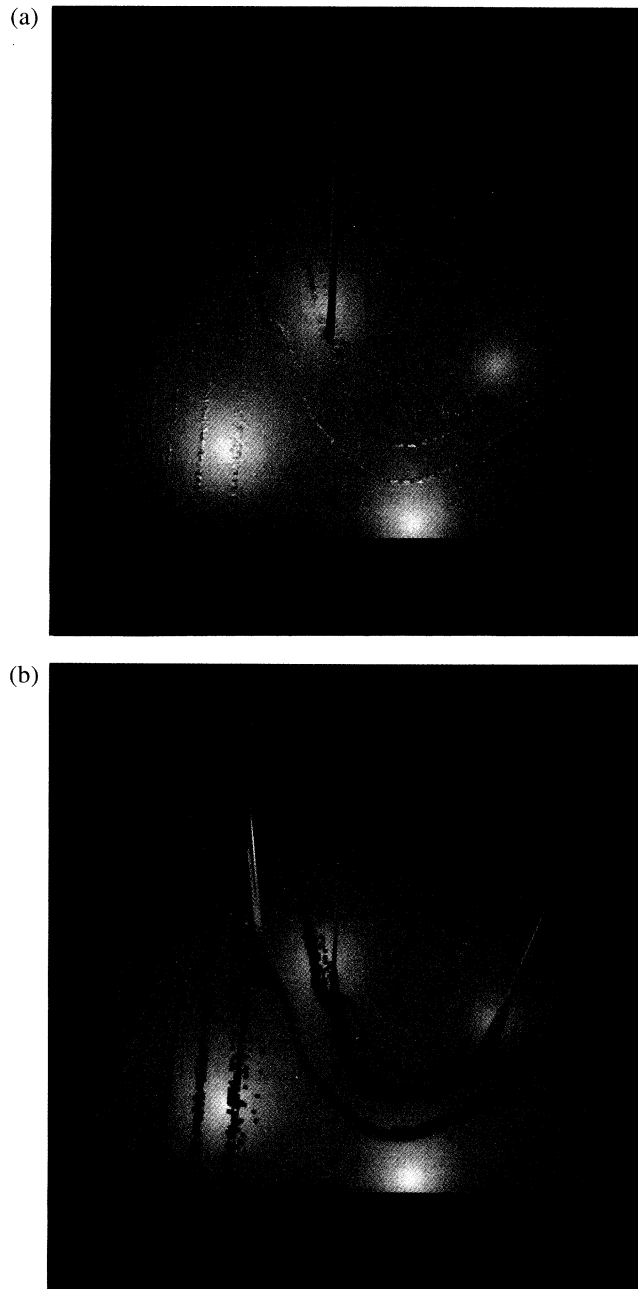


FIG. 4. 3D histograms of (a) the unperturbed and (b) the anticontrolled data distributed over the attractor (return map) of Fig. 1. The scale of (a) is enhanced by a factor of 10 in order to make visible the chaotic transients present in the data. The period 1 peak (which lies on the diagonal line) is so strong that it would be off the scale even had the vertical scale not been enhanced by this factor of 10.

unstable periodic motions that comprise the chaos itself. Hence it is not removed. To reiterate, we interrupt only the

sequence of preiterates that lead to entrapment in a periodic motion. It is because we take this approach, rather than the approach of completely excluding the system for the region of phase space around the unstable periodic motion, that we are able to maintain the chaos with only rare interventions ($\sim 0.12\%$ of the time).

In summary, we have presented a general method for the anticontrol of chaotic systems which is straightforward to implement and need be rarely applied to keep a system chaotic. This method has been demonstrated to work in a magnetomechanical experiment with no failures.

Mark L. Spano is supported by the NSW Independent Research Program and the Office of Naval Research (Division of Physics & Chemistry). W. L. Ditto is supported by the ONR Young Investigator Program.

-
- [1] E. Ott, C. Grebogi, and J. A. Yorke, Phys. Rev. Lett. **64**, 1196 (1990).
 - [2] W. L. Ditto, S. N. Rauseo, and M. L. Spano, Phys. Rev. Lett. **65**, 3211 (1990).
 - [3] R. Roy, T. W. Murphy, T. D. Maier, Z. Gills, and E. R. Hunt, Phys. Rev. Lett. **68**, 1259 (1992).
 - [4] E. R. Hunt, Phys. Rev. Lett. **67**, 1953 (1991).
 - [5] V. Petrov, V. Gaspar, J. Masere, and K. Showalter, Nature (London) **361**, 240 (1993).
 - [6] A. Garfinkel, M. L. Spano, W. L. Ditto, and J. N. Weiss, Science **257**, 1230 (1992).
 - [7] S. J. Schiff, K. Jerger, D. H. Duong, T. Chang, M. L. Spano, and W. L. Ditto, Nature (London) **370**, 615 (1994).
 - [8] For a nice review, see T. A. Shinbrot, C. Grebogi, E. Ott, and J. A. Yorke, Nature (London) **363**, 411 (1993). Also of interest is W. L. Ditto and L. M. Pecora, Sci. Am. **269**, No. 2, 78 (1993).
 - [9] For instance, some studies of heart rate variability suggest that losing complexity in the heart rate will increase the mortality rate of cardiac patients. See, for example, M. A. Woo, W. G. Stevenson, D. K. Moser, R. M. Harper, and R. Trelease, Am. Heart J. **123**, 704 (1992); A. L. Goldberger, Ann. Biomed. Eng. **18**, 195 (1990).
 - [10] J. M. Ottino, Sci. Am. **260**, No. 1, 40 (1989); J. M. Ottino, F. J. Muzzio, M. Tjahjadi, J. G. Franjione, S. C. Jana, and H. A. Kusch, Science **257**, 754 (1992); J. M. Ottino, Guy Metcalfe, and S. C. Jana, in *Proceedings of the 2nd Experimental Chaos Conference* (World Scientific, Singapore, 1995), pp. 3–20.
 - [11] W. Yang, M. Ding, A. Mandell, and E. Ott, Phys. Rev. E **51**, 102 (1995).
 - [12] The statistics associated with the dwell times the system spends in periodic motion are consistent with type III intermittency. For a discussion of intermittency types, see P. Berge, Y. Pomeau, and C. Vidal, *Order Within Chaos* (John Wiley & Sons and Hermann, Paris, 1984).
 - [13] W. L. Ditto, S. Rauseo, R. Cawley, C. Grebogi, G. H. Hsu, E. Kostelich, E. Ott, H. T. Savage, R. Segnan, M. L. Spano, and J. A. Yorke, Phys. Rev. Lett. **63**, 923 (1989).

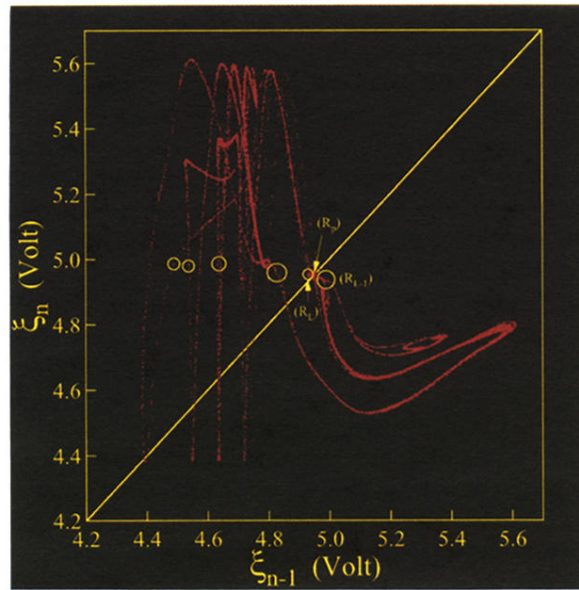


FIG. 1. Return map constructed from experimental data showing the loss region and its preiterates (circles). Region (R_L) denotes the loss region, region (R_{L-1}) denotes the first preiterate of the loss region going back in time, and region (R_p) denotes the period 1 orbits clustering on the diagonal of the map. The other four circles denote the (R_{L-m}) preiterate regions. Any orbit that falls into any one of the R_{L-m} regions will proceed directly into the R_{L-1} region and then proceed onto the loss region followed by the unwanted periodic orbit.

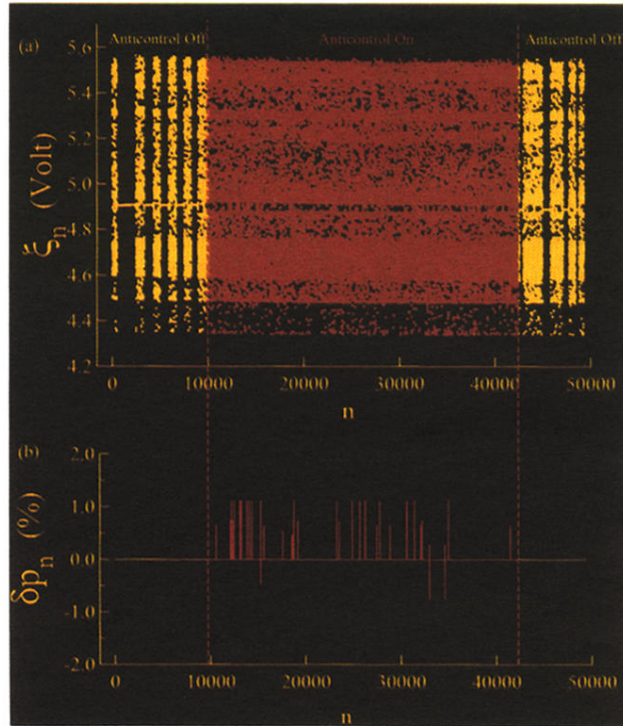


FIG. 2. (a) Time series from experimental data showing the system before, during, and after anticontrol. The dashed vertical lines separate the different regions. Before and after anticontrol, the system is switching between chaos and periodicity (laminar phase). With the perturbations applied during anticontrol, the system is rid of laminar phases. (b) Perturbations applied to achieve anticontrol. Their magnitudes are expressed as a percentage of the nominal dc magnetic field of -1.221 Oe. $\delta p_{\max} = 1.106\%$ and the fraction of time with $\delta p \neq 0$ is 0.0012.

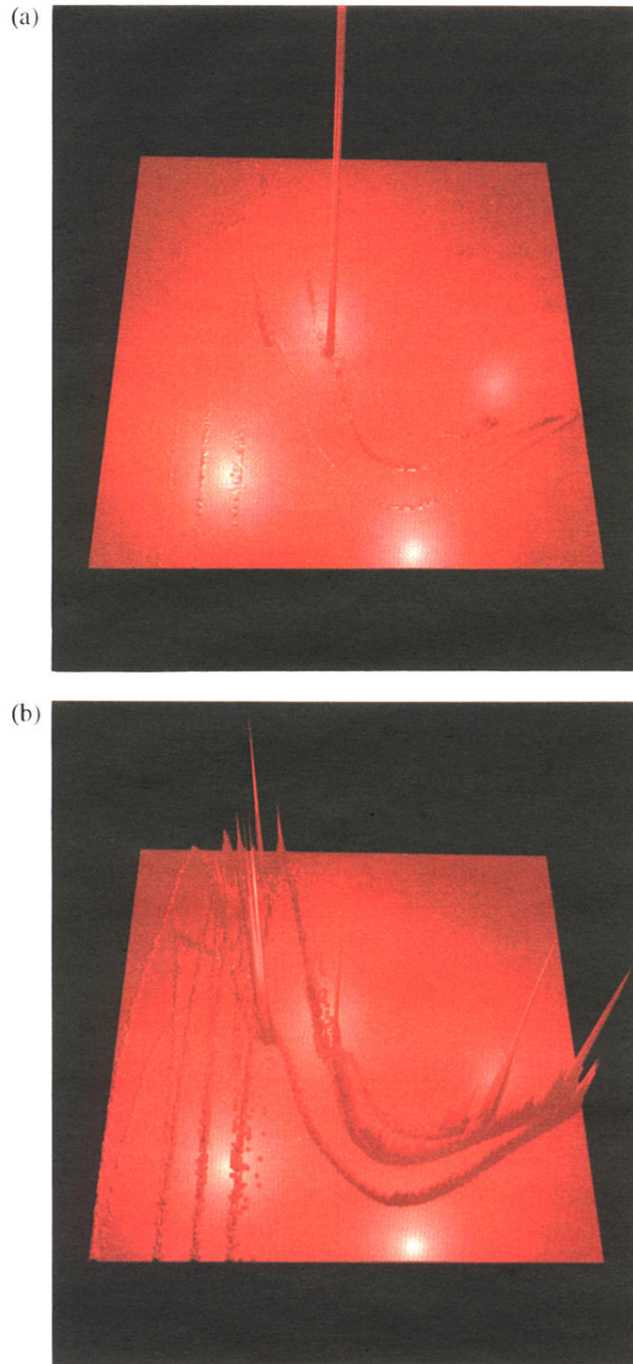


FIG. 4. 3D histograms of (a) the unperturbed and (b) the anticontrolled data distributed over the attractor (return map) of Fig. 1. The scale of (a) is enhanced by a factor of 10 in order to make visible the chaotic transients present in the data. The period 1 peak (which lies on the diagonal line) is so strong that it would be off the scale even had the vertical scale not been enhanced by this factor of 10.